International Journal of Recent Technology and Engineering (IJRTE)
ISSN: 2277-3878 (Online), Volume-8 Issue-4, November 2019

Laterally Extended Field of View Imaging without Geometric Distortion using Image Stitching in Open-Configuration MRI

Cheolpyo Hong, Bong Soo Han

Abstract*: *Open-configuration MRI for easy patient access causes a restricted imaging field of view and geometric distortion resulting in reduced reliability of the quantitation of tissue segmentation. The method proposed in this study is use of MR image stitching, which is merging divided isocentric images without geometric distortion of the same object through the table moving laterally. This study was performed using an open 0.32 T MRI system. MR imaging with lateral shift of the scanner table was conducted using an AAPM MRI Phantom. The composite image produced through the sequential generation of the same object at different table positions has been generated using the image stitching technique. Image stitching consisted of tile configurations using optimized global registration and then seamlessly blending the aligned tiles. The overall image stitching procedure reduced the geometric distortion of image at off-center regions, and the FOV in the stitched image was extended 40% laterally relative to conventional isocenter image. The maximum distortion value was about 16.8 mm in the conventional image and was reduced to < 1.7 mm after the seamless image stitching procedure. Laterally extended FOV without geometric distortion was successfully acquired using seamless image stitching procedure. These methods are beneficial towards defining tissue segmentation in obese patient with large field of view in open MRI.

Index Terms*: *Extended field of view, seamless image, image stitching, geometric distortion, open MRI.

I. INTRODUCTION

Open MRI is suitable for the comfortable imaging without claustrophobia of obese patients and for the use of additional equipment in the positioning required for MRI-based therapy [1-3]. For obese individuals, abdominal imaging is achieved by using deeply penetrating radiofrequency which allows the longitudinal study of obesity without a dose of radiation. The benefits of such MRI is valuable for the assessment of visceral adipose tissue, a risk factor highly related to cardiovascular disease and type 2 diabetes mellitus [4,5]. MR imaging of radiotherapy treatment planning (RTP) has shown superior soft tissue contrast, which can improve the target volume delineation compared to CT [3,6]. Enhanced structure delineation enables accurate and precise chemotherapy dose delivery to tumors.

However, quantification of anatomical information has been affected by a laterally-limited patient aperture and geometrically-distorted images caused by imaging gradient nonlinearity in open-configuration MRI [7,8]. Field of view restriction has led to erroneous estimation of adipose tissue amounts in obese patient and spatial distortion presents a severe obstacle in the use of MRI as a reliable tool for RTP.

In order to extend imaging field of view, image stitching which is widely used in computer vision, such as in mosaic imaging and in the panoramic view is an exciting approach [9-11]. The stitching procedure is the composition of an image through the sequential generation of different views of the same object. Divided images of the same object are aligned by configuration layout, such as the number of images, the image sequence, and the gird size. Merging of a configured image is performed by seamless blending. This allows an intensified field of view and image resolution within a physically restricted imaging aperture. In particular, this stitching procedure which is merging divided isocentric images of the same object may result in an elongated field of view without geometric distortion due to main field homogeneity and gradient field linearity are guaranteed near the isocenter relative to the far from the magnet isocenter in MRI. The purpose of this study was to elongate field of view without spatial distortion-artifact using seamless image stitching. Divided isocentric images of same object were acquired at magnet isocenter and by moving patient table laterally, because imaging gradient is linear near the isocenter. These multiple isocentric images were merged using nonlinear blending.

II. MATERIALS AND METHOD

A. Image acquisitions

MR data acquisitions were performed using an open 0.32 T MRI (Magfinder II, SciMedix Co., Ltd., Korea) with a permanent magnet. The diameter of magnet is 137 cm and resonant frequency is 13.6 MHz. The MR configuration has a patient aperture of 1370 mm and maximum FOV of 400 mm2. The patient table can be laterally moved up to 120 mm relative to the magnet center.

Manuscript published on November 30, 2019.
* Correspondence Author
Cheolpyo Hong*, Department of Radiological Science, Daegu Catholic University, Daegu, Republic of Korea. Email: chong@cu.ac.kr
Bong Soo Han, Department of Radiological Science, Yonsei University, Kwangwon-do, Republic of Korea.

For the estimation of the geometric distortion, MR imaging was carried out on an AAPM (The American Association of Physicists in Medicine) uniformity/linearity phantom (Nuclear Associates, model 76-907) and on one healthy adult. Subject was provided written informed consent.

All procedures and subjects were approved by Yonsei Univesity Wonju Sevrance Christian Hospital institutional review board. The phantom has outer dimensions of 330.2 mm × 330.2 mm × 101.6 mm and the square grid has 285 mm × 285 mm in plane. The grid section coronal images of phantom were acquired with a 2D T1 spin echo(TR = 400 ms, TE = 15 ms, bandwidth = 52.6 Hz, matrix = 256 × 256, FOV = 450 mm, slice thickness = 5 mm). Abdominal images within the coronal planes were acquired with a 2D T1 spin echo following parameter; TR = 475 ms, TE = 15 ms, bandwidth = 52.6 Hz , matrix = 256 × 320, FOV = 450 mm, slice thickness = 10 mm, number of signal average = 3.

B. Distortion measurements and tile configuration

The square grid section of uniformity/linearity phantom contained 2 sheets. The control points were defined grid intersection of a phantom with a total of 882 control points. The spacing between square grids was assumed to be 14 mm in vertical and in horizontal directions. The control points used in this experiment were measured using one sheet at the isocentric plane; some of the 441 control points are demonstrated in Fig. 1. The geometrical distortion in plane was determined as the difference between the coordinates of each corresponding phantom image and the idealized control point.

$$dr = \sqrt{(dx)^2 + (dy)^2}$$

where dx and dy are the difference between measured and idealized defined position. In addition to calculating distortion at each point in a frame of reference, the distortion value measured as a function of radial distance from isocenter in plane. This value was used to set acceptable distortion value. The acceptable distortion value in this experiment defined < 2 % along the radial distance and acceptable distortion area, called image tiles, has a size 125 mm of lateral distance. The number of image tiles depends on the size of the subject imaged, the size of the image tile and the overlapping ratio of the two neighboring image tiles.

Considering that the phantom size was 285 mm and image tile size was 125 mm, three image tiles were enough to cover the whole phantom with an appropriate overlapping ratio within the range of 15% to 30%. For this overlapping ratio, the first image acquired at conventional isocenter followed by the others to move a table in a 90 mm on the left and in the right direction (see Fig. 2 top row).

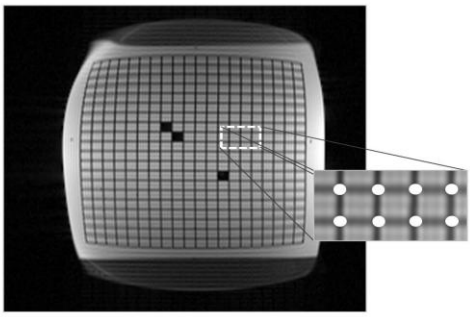

Figure 1. The AAPM phantom images acquired at the isocentric plane

C. Seamless Image stitching

The image stitching method used in this study consisted of image configuration using optimized global registration and seamless blending of aligned images [12]. The initial image alignment was performed on a pair-wise basis for all the overlapping parts of the neighboring tiles. The global optimization was processed over the alignment by balancing the differences of the pair-wise correlations and minimizing the sum of least squares of all variations from the superposition areas, calculated by the phase correlation. Phase correlation is derived from Fourier-based approach that the Fourier transformation (FT) of translational offsets between images results in a linear phase difference. Two image f(x) and g(x) are related by translational difference, the offset can be computed form the cross power spectrum R(u) of both images,

$$R(u) = \frac{F(u)G(u)^*}{|F(u)G(u)^*|}$$

where, $F(u)$ = FT[f(x)], $G(u)$ = FT[g(x)] and * denotes complex conjugate. To avoid unsuitable cross correlation, the acceptable tile configuration was set within the predefined ratio between the maximal and average displacement. Seamless manner of aligned image was performed by an alpha blending function. The weighted non-linear method has been applied, considering that the overlapping area of the images was inconsistent in brightness. The weighting map was created by the exponential decrease of the brightness from the isocentric point of the image.

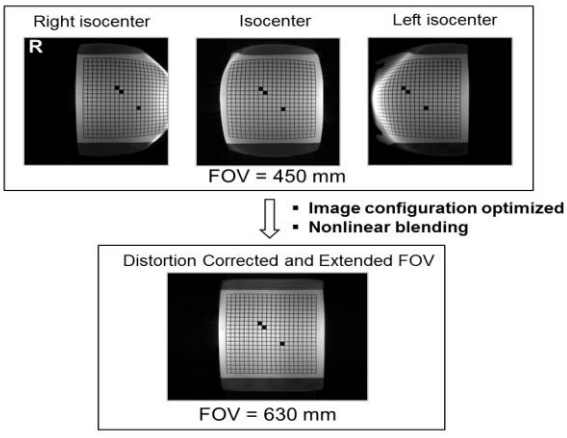

Figure 2. The overall image stitching procedure

III. RESULTS

Fig. 2 shows 3 coronal images and the stitching procedure of divided isocenter images. For each image shown in the top row of Fig. 2, the image showed a larger distortion over peripheral region compared with the near isocenter. The left isocenter image moved in right direction, showed right region of phantom severely distorted. The distortion of right isocenter image was similar to that shown in left isocenter image, symmetric with respect to vertical line of isocenter The overall image stitching procedure reduced the geometric distortion of image at off-center regions, and the field of view in the stitched image was extended 40% laterally relative to conventional isocenter image. Shown in Fig. 3c are spatial positions of the control points measured in isocentric plane. The hollow circles indicate control points in Fig. 1, and the solid is corresponding points of the stitched image. The control point was assumed to be 14 mm apart. As expected, the stitched image shows little distortion. Fig. 3d illustrates the radial distortion value from the isocenter. The maximum distortion value was about 16.8 mm in the conventional image and was reduced to < 1.7 mm after the stitching procedure.

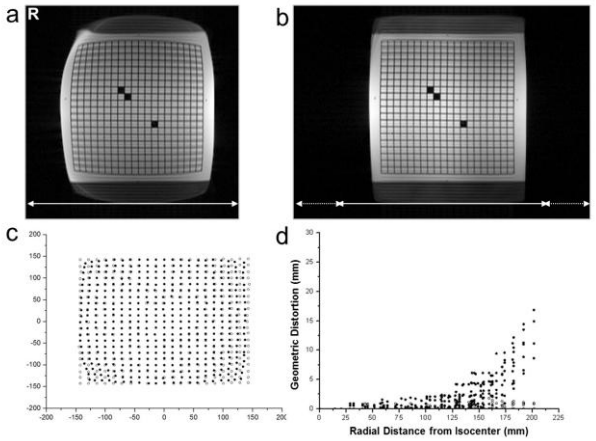

Figure 3. Comparison of conventional image and stitched image

Fig. 4 shows an example of stitched and conventional abdominal image acquired at coronal plane of torso. The conventional isocenter image showed large distortion at the peripheral regions of the coronal image in comparison to that of the stitched image. Geometrical distortion of the outer region was significantly reduced at stitched image. The stitched mosaic image was extended 20% laterally relative to conventionally scanned image.

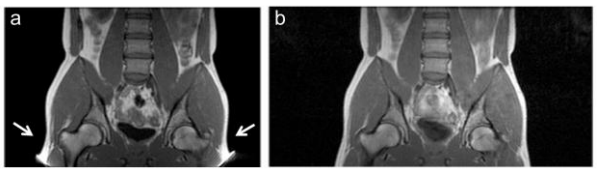

Figure 4. The stitching results procedure of coronal images for human abdomen

IV. DISCUSSION

Laterally extended field of view without geometric distortion was successfully acquired using seamless image stitching. The stitching procedure, which is widely used in photography, is suitable to extend field of view in MRI. In previous image stitching approach, the resultant configured image is slightly misaligned without precise arrangement of tiles and this imprecise link causes blurring of an object. In this study, residual error of moving the image plane was compensated within globally optimized configuration manner, and the undistorted image was acquired using nonlinear blending of configured images.

The major advantage of proposed methods is that the FOV extending is not limited by the distortion correction methods and can be applied to unlimited extend field of view without distortion, shown in Fig 3. Geometrical distortion corrections have been intensively studied in longitudinal morphometric study and in radiotherapy simulation or planning [13-15]. Correction methods described in previous studies include spherical harmonic deconvolution of the magnetic field and the phantom mapping-based correction approach [16-19]. The magnetic field which is modeled using spherical harmonic expansion of the imaging gradient represents the geometrical characteristic of gradient coil; these spherical harmonic coefficients can be used to correct spatial distortion. Phantom image-based correction uses the interpolation method for variation of spatial distortion and the resultant residual distortion of this approach is highly suppressed compared to the spherical harmonic expansion method. However, the above methods are limited in their direct implementation in a larger field of view in open-configuration system which has a larger lateral dimension. Moreover, the specially designed heave phantom and the complicated processing are needed to evaluate distortion.

The characteristic of the MRI gradient system is that gradient linearity is guaranteed on and near the isocenter relative to far from center. This allows a large field of view imaging through the multiple isocentric images merging without particular distortion correction methods. Moreover, geometrical distortion caused by imaging gradient nonlinearity at the peripheral region is not object-related distortion, but system-induced distortion. Image stitching of segmented isocenter image with predefined distortion free area efficiently decreases such hardware imperfections.

Considering that the distortions are very small near to isocenter, although the ‘ground truth’ of abdomen is not known, seamless stitching method reduced the geometric distortion with larger coverage of resultant image, shown in Fig. 4. The tissue quantify can be measured precisely and accurately in stitched image compared with the conventional image. Moreover, this distortion suppression image with large FOV may be beneficial for planning treatment, which requires accurate depiction of a patient skin contour. The motion artifact caused by the internal organ movement is negligible because of seamless blending with non-linear weighting map and does not have an effect on visual inspection shown in Fig 4. Increased examination time acquiring more images, the limitation of this study, is reduced by parallel imaging technique with phase-arrayed coil and reduced FOV imaging MR sequence.

V. CONCLUSION

This study demonstrated laterally extended FOV imaging without geometric distortion using seamless image stitching in open-configuration MRI. These approaches are beneficial towards delineating tissue margin in patient with large FOV in open MRI.

ACKNOWLEDGMENT

This work was supported by research grants from the Daegu Catholic University in 2017(20171056)

REFERENCES

1. Rothschild PA, Domesek JM, Eastham ME, Kaufman L (1991) MR imaging of excessively obese patients: the use of an open permanent magnet. Magn Reson Imaging 9: 151-154.
2. de Bucourt M, Streitparth F, Wonneberger U, Rump J, Teichgraber U (2011) Obese patients in an open MRI at 1.0 Tesla: image quality, diagnostic impact and feasibility. Eur Radiol 21: 1004-1015.
3. Krempien RC, Schubert K, Zierhut D, Steckner MC, Treiber M, et al. (2002) Open low-field magnetic resonance imaging in radiation therapy treatment planning. Int J Radiat Oncol Biol Phys 53: 1350-1360.
4. Gronemeyer SA, Steen RG, Kauffman WM, Reddick WE, Glass JO (2000) Fast adipose tissue (FAT) assessment by MRI. Magn Reson Imaging 18: 815-818.
5. Donnelly LF, O'Brien KJ, Dardzinski BJ, Poe SA, Bean JA, et al. (2003) Using a phantom to compare MR techniques for determining the ratio of intraabdominal to subcutaneous adipose tissue. American journal of roentgenology 180: 993-998.
6. Debois M, Oyen R, Maes F, Verswijvel G, Gatti G, et al. (1999) The contribution of magnetic resonance imaging to the three-dimensional treatment planning of localized prostate cancer. International Journal of Radiation Oncology, Biology, Physics 45: 857-865.
7. Fransson A, Andreo P, Pötter R (2001) Aspects of MR image distortions in radiotherapy treatment planning. Strahlentherapie und Onkologie 177: 59-73.
8. Kullberg J, Brandberg J, Angelhed J-E, Frimmel H, Bergelin E, et al. (2009) Whole-body adipose tissue analysis: comparison of MRI, CT and dual energy X-ray absorptiometry. British Journal of Radiology 82: 123-130.
9. Chen C-Y, Klette R. Image stitching—Comparisons and new techniques; 1999. Springer. pp. 615-622.
10. Levin A, Zomet A, Peleg S, Weiss Y (2004) Seamless image stitching in the gradient domain. Computer Vision-ECCV 2004: Springer. pp. 377-389.
11. Brown M, Lowe DG (2007) Automatic panoramic image stitching using invariant features. International Journal of Computer Vision 74: 59-73.
12. Preibisch S, Saalfeld S, Tomancak P (2009) Globally optimal stitching of tiled 3D microscopic image acquisitions. Bioinformatics 25: 1463-1465.
13. Mah D, Steckner M, Palacio E, Mitra R, Richardson T, et al. (2002) Characteristics and quality assurance of a dedicated open 0.23 T MRI for radiation therapy simulation. Medical physics 29: 2541.
14. Chen Z, Ma C, Paskalev K, Li J, Yang J, et al. (2006) Investigation of MR image distortion for radiotherapy treatment planning of prostate cancer. Physics in medicine and biology 51: 1393.
15. Jovicich J, Czanner S, Greve D, Haley E, van der Kouwe A, et al. (2006) Reliability in multi-site structural MRI studies: effects of gradient non-linearity correction on phantom and human data. Neuroimage 30: 436-443.
16. Wang D, Strugnell W, Cowin G, Doddrell DM, Slaughter R (2004) Geometric distortion in clinical MRI systems: Part I: evaluation using a 3D phantom. Magnetic resonance imaging 22: 1211-1221.
17. Wang D, Strugnell W, Cowin G, Doddrell DM, Slaughter R (2004) Geometric distortion in clinical MRI systems: Part II: correction using a 3D phantom. Magnetic resonance imaging 22: 1223-1232.
18. Janke A, Zhao H, Cowin GJ, Galloway GJ, Doddrell DM (2004) Use of spherical harmonic deconvolution methods to compensate for nonlinear gradient effects on MRI images. Magnetic resonance in medicine 52: 115-122.
19. Wang D, Doddrell DM, Cowin G (2004) A novel phantom and method for comprehensive 3-dimensional measurement and correction of geometric distortion in magnetic resonance imaging. Magnetic resonance imaging 22: 529-542.

AUTHORS PROFILE

Cheolpyo Hong, Assistant Professor, Department of Radiological Science, Daegu Catholic University, Daegu, Republic of Korea

Dr. Hong has received Ph.D. in MRI sequence and geometric distortion correction from Yonsei University, Kwangwon-do. His research interests are MRI guided radiation therapy and Quantitative Imaging. He has 10 years of Teaching Experience in Radiological Science and Published 25 articles in various journals and international conferences.

Bong Soo Han, Professor, Department of Radiological Science, Yonsei University, Kwangwon-do, Republic of Korea. Dr. Han has received Ph.D. in Nuclear Physics from Yonsei University, Seoul. His research interest is Diffusion Tensor Imaging for neurological disease, especially multiple sclerosis. He has 25 years of Teaching Experience in Radiological Science and Published 45 articles in various journals and international conferences.